Characterization of Dimyristoylphosphatidylcholine Vesicles and Their Dimensional Changes through the Phase Transition: Molecular Control of Membrane Morphology†

Anthony Watts,* Derek Marsh, and Peter F. Knowles

ABSTRACT: The molecular control of vesicle size, on passage through the ordered-fluid bilayer phase transition, has been studied using phosphatidylcholine single-bilayer vesicles. Vesicles of dimyristoylphosphatidylcholine were prepared by sonication above the phase transition and fractionation by centrifugation. The vesicles were characterized with respect to homogeneity, shape, partial specific volume, sedimentation velocity, diffusion coefficient, intrinsic viscosity, and internal volume, using column chromatography, electron microscopy, analytical ultracentrifugation, capillary-flow viscometry and spin-label trapped volume determinations. Measurements at various temperatures through the lipid phase transition indicate that the vesicles remain spherical and constant in lipid content with an anhydrous molecular weight of $1.93 \pm 0.10 \times 10^6$, corresponding to 2850 ± 140 lipid molecules per vesicle, but undergo large changes in dimensions and hydration. On going from 15 to 30 °C the vesicle's outer radius increases from 96.8 ± 2.9 to 127.8 ± 2.8 Å, the internal volume increases from 0.107 ± 0.024 to 0.639 ± 0.005 mL/g lipid and the bound water increases from 0.091 ± 0.061 to 0.580 ± 0.037 g/g lipid. These changes are controlled by the molecular events occurring in the lipid bilayer which are characterized by a thinning of the bilayer from 50.7 ± 0.5 Å at 15 °C to 29.8 ± 1.3 Å at 30 °C, accompanied by a lateral expansion in area/molecule from 45.3 ± 3.6 Å^2 to 74.7 ± 3.7 Å^2 and an increase in partial specific volume from 0.9328 ± 0.0014 to $.9726 \pm 0.0014$ mL/g. One of the most dramatic changes found is the sixfold increase in internal volume, which could have important functional consequences arising from the change in concentration of internal solutes. Other important functional changes could also arise from the increase in surface area and bound water.

The central part played by the phospholipid bilayer in the structure of biological membranes is now well-recognized (for reviews, see, e.g., Lee, 1975; Marsh, 1975), and the functional significance of its structural state has been demonstrated in several cases (for a review, see, e.g., Melchior & Steim, 1976). The underlying property of phospholipids which accounts for this important structural role, and which also gives rise to the usefulness of phospholipid bilayers as model membrane systems, is their ability to organize spontaneously into bilayer structures when dispersed in water. Two 0ain types of phospholipid bilayer preparations are currently in use in biophysical and biochemical studies. The first is the extended multi-bilayer dispersion which can be used either as liposomes (Bangham et al., 1974) or as flat, oriented bilayers (see, e.g., Levine & Wilkins, 1971; Schreier-Muccillo et al., 1973). The second is the homogeneous, small, single-bilayer vesicle preparation described by Huang (1969).

The single-bilayer vesicle preparation is particularly advantageous for quantitative studies which require a homogeneous vesicle population with well-defined surface area and internal volume, for example, studies of ligand binding and surface groups (Huang & Charlton, 1972; Huang et al., 1970), vesicle hydration (Newman & Huang, 1975), permeability coefficients (Marsh et al., 1976; Papahadjopoulos & Kimelberg, 1973), phospholipid transfer (Martin & MacDonald, 1976; Papahadjopoulos et al., 1976), or vesicle fusion (Taupin & McConnell, 1972). Studies of vesicle morphology and size also require fully characterized, homogeneous preparations. We have previously performed studies of this type by characterizing the effects of vesicle size in limiting the cooperativity of the ordered-fluid bilayer phase transition and, hence, demonstrating the possibility that membrane morphology can control functional properties of the membrane at the molecular level (Marsh et al., 1977). In the present work we have performed the converse studies of investigating the effects of the bilayer phase transition on vesicle shape and size. These studies show that the phase transition can exert a molecular control on vesicle morphology and hence possibly on cellular function.

We have prepared homogeneous, single-bilayer vesicles composed of DMPC[1] and completely characterized the preparation with respect to vesicle shape, size, molecular weight, and hydration using electron microscopy, analytical ultracentrifugation, trapped volume, and viscosity measurements. This preparation should thus be applicable to all the above-mentioned studies and has already been used in permeability measurements (Marsh et al., 1976) and investigations of the effects of vesicle size on the cooperativity of the phase transition (Marsh et al., 1977). Previous vesicle preparations, which have been characterized in detail, have mostly involved lipids of a single phospholipid type but with hydrocarbon chain heterogeneity (Huang, 1969; Huang & Charlton, 1971; Newman & Huang, 1975). Although applicable to most of the studies mentioned above, preparations with heteroge-

† From the Max-Planck-Institut für biophysikalische Chemie, D-3400 Göttingen, West Germany (A.W. and D.M.), and the Astbury Department of Biophysics, Leeds University, Leeds, LS2 9JT, England (P.F.K.). *Received April 29, 1977; revised manuscript received December 21, 1977.* A preliminary account of this work was presented at the IUB Tenth International Congress of Biochemistry, Hamburg 1976 (Abstract 05-1-272).

[1] Abbreviations used are: DMPC, L-α-dimyristoylphosphatidylcholine: Tempocholine, *N,N*-dimethyl-*N*-(2′,2′,6′,6′-tetramethyl-4′-piperidinyl-1′-oxyl)-2-hydroxyethylammonium; Tempophosphate, 4-hydroxy-2,2,6,6-tetramethylpiperidinyl-1-oxy dihydrogen phosphate ester: Tempo, 2,2,6,6-tetramethylpiperidinyl-1-oxy; ESR, electron spin resonance; Tris, 2-amino-2-hydroxymethyl-1,3-propanediol; SE, standard error.

0006-2960/78/0417-1792$01.00/0

neous chains are less suitable for investigations involving detailed comparisons with the molecular properties of the component lipids, especially those involving bilayer phase transitions. The present preparation is composed solely of DMPC, a phosphatidylcholine with C-14 chains, and has a well-defined ordered-fluid bilayer phase transition centered around 22 °C.

This DMPC vesicle preparation has been used to investigate the changes in vesicle dimensions and morphology through the lipid phase transition. It is found that the vesicles retain their spherical shape, but the vesicle internal and external dimensions and bound water increase dramatically as the bilayer thins and expands laterally on going through the phase transition. The possible implications for cellular and membrane function can be seen from the fact that the internal volume of the vesicle *increases by a factor of 6* on going through the bilayer phase transition. In addition the bound water increases approximately tenfold and the vesicle area increases by 60%.

Experimental Section

Materials. L-α-Dimyristoylphosphatidylcholine (DMPC) was obtained from Fluka, Buchs, Switzerland, and Sigma, St. Louis, Mo. (chromatographically pure, grade I, various Lot numbers). The purity of each lot was checked by thin-layer chromatography and gas–liquid chromatography as previously described (Marsh et al., 1976).

Tempocholine chloride was prepared according to the method of Kornberg & McConnell (1971), by Dr. R. P. Gregson in the Biophysics Department, Leeds University. Tempophosphate was obtained from Syva, Palo Alto, Calif.

Deionized, glass-distilled water was used in all solutions. For the experiments performed with D_2O–H_2O buffered solutions, D_2O (approximately 98% pure, Fisons, U.K.) was added to a tenfold concentrated H_2O buffer solution of 1 M KCl/0.1 M Tris-HCl at pH 8.0. To make the required volume:volume D_2O–H_2O solution, H_2O was added and the pH–pD was adjusted to compensate for the different H^+ and D^+ activities (Bates, 1965). The buffer solution used throughout this work was 0.1 M KCl/0.01 M Tris-HCl at pH 8.0.

Vesicle Preparation. Dry DMPC was dispersed in buffer and sonicated above 23 °C and then centrifuged at 105 000*g* for 10 min at 4 °C as previously described (Marsh et al., 1976, 1977). Lipid phosphate determinations (Dittmer & Lester, 1964) showed that not more than 10% of the originally dispersed lipid was removed during the preparation of the clear vesicle supernatant. Thin-layer chromatography of the extracted lipid ($CHCl_3$–CH_3OH; 2:1 v/v) showed no products of lipid degradation.

Column Chromatography. A 2-mL DMPC vesicle suspension at a concentration of 25 mg mL^{-1} in buffer was fractionated by upward flow on a Sepharose 2B column, 50 × 2.5 cm, jacketed at 32 °C and previously equilibrated with buffer. Fractions of 3 mL were collected and their absorbance at 300 nm was measured with a Unicam SP500 spectrophotometer, at room temperature; approximately 20 °C.

Electron Microscopy. Droplets of 5 mg mL^{-1} vesicle suspension, preincubated at the required temperature, were rapidly frozen in liquid Freon 22. The droplets were cleaved and then etched for the minimum amount of time possible, usually 12–15 s, in a NGN 680 freeze-etch apparatus. Electron micrographs of the freeze-etch replicas were obtained on a Phillips EM 200 microscope and the vesicle diameters measured from their shadow width on projected negatives, enlarged 20×. Vesicles clearly larger than 500 Å in diameter were not measured, these being less than 10% in number of the total population. These somewhat larger vesicles had a single bilayer; no extended multibilayer structures were seen.

Analytical Ultracentrifugation. Sedimentation velocities and diffusion coefficients were measured using a Beckman Model E analytical ultracentrifuge, equipped with an RTIC temperature control unit, controlling the rotor temperature to ±0.1 °C. An An-D rotor and schlieren optical system were used for all measurements.

(a) Sedimentation Coefficients and Partial Specific Volume. Rotor speeds between 36 000 and 50 000 rpm were used for sedimentation runs. Two samples of different concentrations were run simultaneously in two double-sector, capillary-type, synthetic boundary cells, each with a 12-mm optical path. The cell containing the higher vesicle concentration was fitted with a 1° wedge window when the vesicles sedimented and vice-versa when the vesicles floated, giving an inverted schlieren pattern (Hill & Cox, 1965). Measurements of schlieren pattern peak positions were made with a traveling microscope.

Sedimentation coefficients, s, were calculated from linear plots of log r vs. time, where r is the distance from the center of rotation to the point of maximum ordinate of the schlieren pattern (Schachman, 1957). Values of s were extrapolated to give s^0 at zero vesicle concentration, using a linear least-squares fit of the concentration dependence. Quoted $s^0_{20,w}$ values are corrected for the density and viscosity of the various buffered solutions used, by reducing to water at 20 °C, according to the relationship: $s^0_{20,w} = s^0\eta_r(1 - \phi\rho_{20,w})/(1 - \phi\rho)$ where ρ is the density of the suspending solution at temperature T, η_r is its viscosity relative to η_0, the viscosity of water at 20 °C, and $\rho_{20,w}$ is the density of water at 20 °C.

Values of the effective partial specific volume, ϕ, of the DMPC vesicles were determined from the isodensity points in D_2O–H_2O mixtures. From the equation for sedimentation: $\eta_r s^0 = (1 - \phi\rho)M/N\eta_0 f'$; the effective partial specific volume is given by $\phi = 1/\rho_i$, where ρ_i is the intercept at which $\eta_r s^0 = 0$ (Huang & Charlton, 1971).

(b) Diffusion Measurements. Diffusion studies were carried out under conditions similar to those for the sedimentation runs, except that rotor speeds of between 6000 and 9000 rpm for 1–2 h were used. At these speeds the concentration boundary did not move appreciably. Apparent diffusion coefficients, D, were calculated by the maximum ordinate–area method (Ehrenberg, 1957), using the relationship: $D = (\frac{1}{4}\pi t)[A/kH_{max}]^2$, where k is the magnification factor along the radial coordinate and t is the time in seconds between boundary formation and the photograph being taken. A is the area under the schlieren peak, determined by weighing the enlarged image of the schlieren pattern and H_{max} is the maximum height of the same enlarged image. This method of diffusion coefficient measurement is still applicable to partially inhomogeneous solutes (Chervenka, 1969), although the actual patterns obtained in the experiments were fairly symmetrical. Apparent diffusion coefficients were extrapolated to infinite dilution to give D^0 values which were then reduced to values in water at 20 °C, according to the relationship, $D^0_{20,w} = D^0\eta_r(293/T)$, where T is in Kelvin degrees.

Viscosity and Density Measurements. The intrinsic viscosities of the vesicle suspensions and the relative viscosities of the suspending buffer (for the $s^0_{20,w}$ and $D^0_{20,w}$ corrections) were determined using an Ostwald viscometer with a volume of 3 mL, capillary diameter of 0.3 mm and water flow time of 254 s at 20 °C. The viscometer was previously coated with a 0.5-mg mL^{-1} poly(L-arginine) solution in 0.5 M Tris (pH 7.0) to neutralize the ζ potential of the viscometer glass (Newman & Huang, 1975). The viscometer was suspended in a water bath thermostated at the required temperature to an accuracy

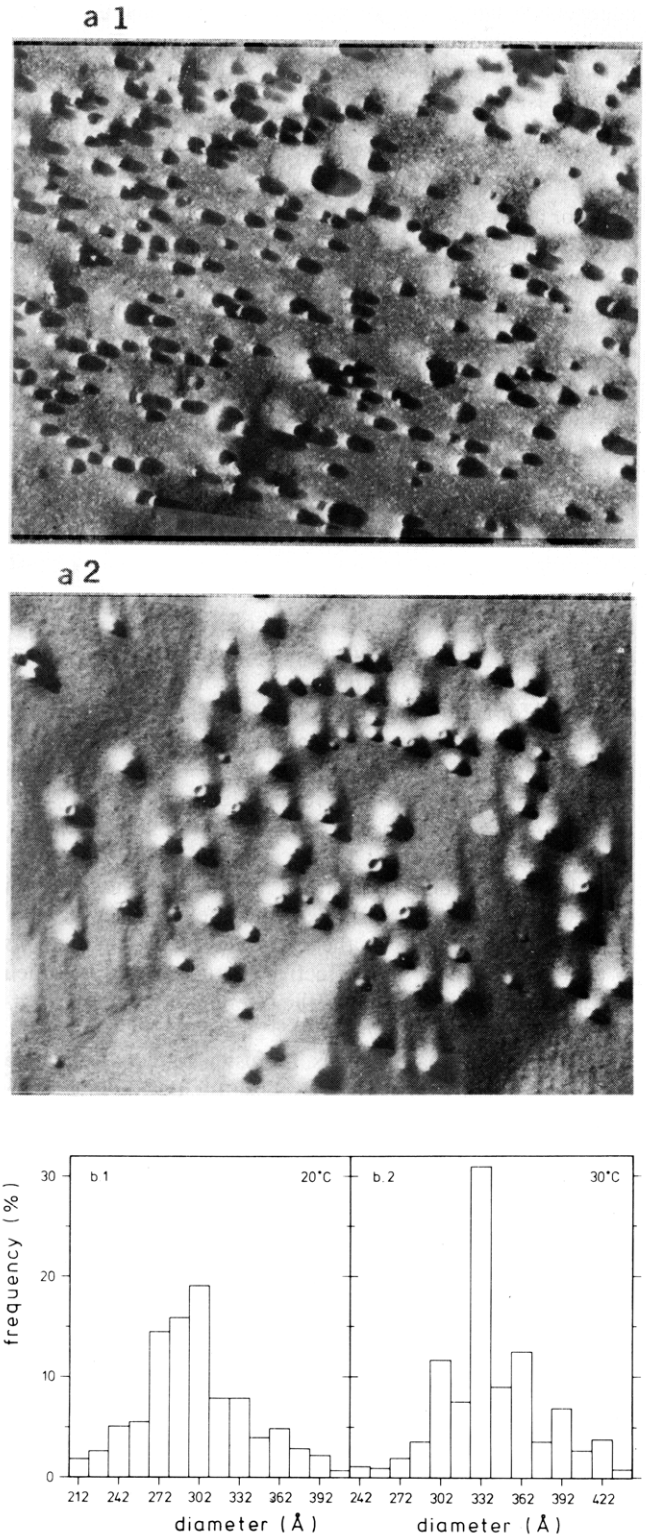

FIGURE 1: (a) Freeze-etch electron micrographs of DMPC vesicles frozen from (1) 20 °C and (2) 30 °C (magnification × 49 500). (b) Histograms of DMPC vesicle diameters measured from freeze-etch micrographs of vesicles quenched from (1) 20 °C (634 vesicles measured) and (2) 30 °C (809 vesicles measured).

of ±0.05 °C. Flow times were the average of more than ten measurements, all within ±0.4% of each other, measured by eye using a stopwatch. The viscosities of D_2O–H_2O buffered solutions at a particular temperature were calculated relative to that of water at 20 °C from the relationship $\eta_r = td/t_w d_w$, where the subscript w refers to water at 20 °C and t and d are the flow time and density of the solution, respectively.

Flow times of DMPC vesicles in H_2O-buffered solutions were measured on serial dilutions of a stock ~15 mg mL^{-1} vesicle sample. Vesicle samples were removed from the viscometer after a set of measurements for concentration determination by phosphate analysis (Eibl & Lands, 1969). Intrinsic viscosities of the vesicle suspensions were obtained from plots of η_{sp}/c vs. c, where η_{sp} is the specific viscosity and c the lipid concentration (Huggins, 1942).

The densities of the suspending media were determined using a 10-mL pycnometer with a capillary neck. Standardization of the pycnometer volume at each temperature was made using distilled water. Measurements were the average of at least ten weighings, made using an Oertling balance reading to ±0.0001 g.

Trapped Volume Measurement. The internal volume of DMPC vesicles was measured by ESR after incubation of the vesicles with the Tempocholine spin label for 2 h and subsequent ascorbate treatment, as described previously (Marsh et al., 1976). The trapped volume is then given by: $v_c = h/(h_0 c_1)$ where h, h_0 are the line heights of the ascorbate-treated and control samples, respectively, and c_1 (g/mL) is the final lipid concentration of the sample.

It has previously been shown that complete equilibration of Tempocholine across the bilayer occurs after incubation for 2 h at temperatures above 17 °C (Marsh et al., 1976). As a control, cosonication of vesicles with Tempocholine at 30 °C gives a trapped volume identical with that obtained by permeability measurements, as also does cosonication with Tempophosphate, an ionic spin label of opposite charge.

Since DMPC vesicles are not appreciably permeable to Tempocholine below 17 °C (Marsh et al., 1976) the Tempocholine was equilibrated across the bilayer by a brief resonication at the required temperature. A vesicle sample, prepared as for the permeability–equilibration method, was contained in a thermostated vessel and resonicated in 30-s bursts for a total period of 10 min. The temperature of the vesicle suspension was monitored by a thermocouple positioned close to the sonicator tip and was controlled to within ±0.5 °C by attenuating the sonicator power. The sonicator power was adjusted so that local sonicator tip heating caused a 4 °C increase in the vesicle sample temperature above the temperature of the recirculating water of the thermostated sonication vessel. After resonication, the vesicle internal volume was measured in exactly the same way as described above. The kinetics of uptake by this method were also studied to ensure that complete equilibration across the bilayer was obtained after a 10-min period. As a further control, it was found that the resonication method gave results identical with those from the permeability–equilibration method at temperatures above 17 °C.

Results

Column Chromatography. The elution profile for DMPC vesicles fractionated on Sepharose 2B was essentially the same as that obtained previously (Marsh et al., 1976), essentially consisting only of Huang's peak II, single-bilayer vesicle fraction (Huang, 1969). Thus the sonication and high-speed centrifugation procedure used here produces a lipid dispersion composed almost entirely of a homogeneous population of single-bilayer vesicles, with very little contamination by large multilamellar vesicles (see also below). It was found that the material after chromatography had a higher optical turbidity than would be expected from small single-bilayer vesicles (Chong & Colbow, 1976; Marsh et al., 1977), indicating that

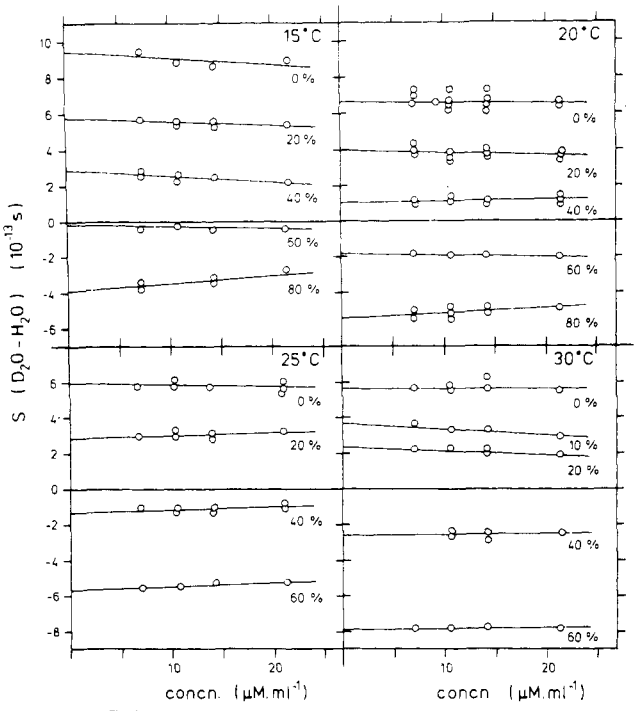

FIGURE 2: Sedimentation coefficients vs. concentration of DMPC vesicles suspended in various D_2O–H_2O buffer mixtures at different temperatures. Figures in % refer to volume % of D_2O in the 0.1 M KCl/0.01 M Tris (pH 8.0) buffer.

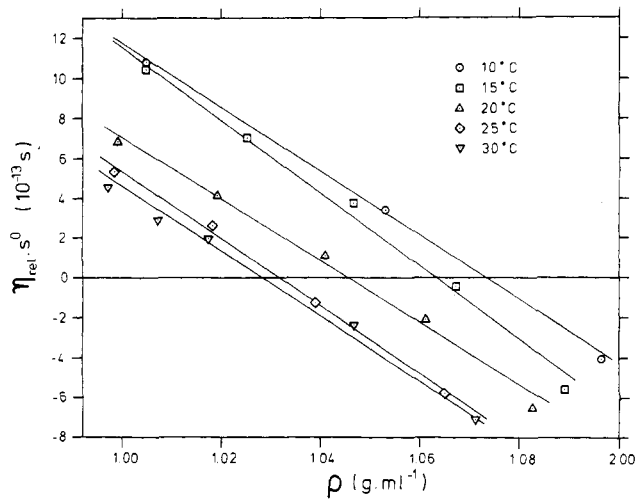

FIGURE 3: Viscosity-corrected sedimentation coefficients, $\eta_r s^0$, for DMPC vesicles at various temperatures, vs. density of the suspending D_2O–H_2O KCl/Tris (pH 8.0) buffer.

some aggregation or collapsing of the vesicles into larger structures had taken place in the latter stages on the column. In addition, the chromatographed vesicles were found to be particularly unstable to reconcentration after chromatography, again producing larger structures. This finding was confirmed by rechromatography of the vesicles under identical conditions, in which case a considerable void-volume peak composed of larger vesicles was detected. Consequently, all the measurements which follow were performed on homogeneous vesicle preparations produced by the sonication procedure described above and fractionated only by the high-speed centrifugation step.

Electron Microscopy. Typical freeze-etch electron micrographs of vesicle samples quenched from temperatures above and at the lower end of the phase transition of DMPC are given in Figure 1a. These show that the vesicles are spherical, are composed of a single bilayer, and have a hollow central compartment. The frequency of occurrence of cross-cleaved vesicles is low in these micrographs because of the difficulty in etching for a sufficiently short time that only cleaved vesicles are exposed. Mostly vesicles which have not been cleaved but are exposed by etching are seen.

The histograms of the distribution of measured vesicle diameters are given in Figure 1b for vesicles quenched from temperatures of 30 and 20 °C. More than 600 diameters at both temperatures (see Figure 1) were measured and these only from vesicles which are clearly exposed by etching, to avoid skewing the size distribution to smaller diameters by the presence of only partly exposed vesicles. The observed distributions are relatively narrow with standard deviations in the vesicle radii of 20.1 ± 0.56 Å (SE, n = 634) for the vesicles quenched from 20°C and 18.3 ± 0.45 (SE, n = 809) for those quenched from 30 °C. This confirms that the vesicle populations are reasonably homogeneous with a well-defined mean radius.

The mean radii of the distributions are 149.6 ± 0.64 Å (SE, n = 634) for the 20 °C vesicles and 171.1 ± 0.79 Å (SE, n = 809) for the 30 °C vesicles. These values are approximately 40–50 Å greater than those obtained by the hydrodynamic measurements described below. The difference may be due to the thickness of the shadowed platinum–carbon replica and, possibly, also to unetchable salt eutectic formed on the surface of the vesicle. However, it is clear from Figure 1b that the mean radius of vesicles quenched from 30 °C is approximately 20 Å greater than that of those quenched from 20 °C. This value should not be too sensitively dependent on replica and eutectic thickness for equivalent preparation procedures, and compares reasonably well with the increase in outer radius of approximately 30 Å between 20 and 30 °C obtained in the hydrodynamic experiments described below. Apparently the difference in lipid hydrocarbon chain conformation above the phase transition can be frozen-in in much the same way as is observed for extended multibilayer vesicles (see, e.g., Kleeman & McConnell, 1976). This conclusion is supported by the fact that vesicles quenched from 25 °C had a similar standard deviation of 17.1 ± 0.67 Å but mean radius of 164.6 ± 0.95 Å, intermediate between the 20 and 30 °C values.

Sedimentation Velocity and Partial Specific Volume. All schlieren sedimentation patterns were found to be reasonably symmetrical and in particular no greater degree of asymmetry was observed at temperatures below the phase transition than was seen above. Measurements on a number of schlieren patterns showed that the leading edges were larger than the trailing edges by no more than 9–14% of the total pattern area. This indicates that the vesicle population is reasonably homogeneous, in agreement with the electron microscopy and column chromatography results.

The concentration dependencies of the sedimentation coefficients of DMPC vesicles, suspended in various D_2O–H_2O buffered solutions at different temperatures throughout the phase transition, are given in Figure 2. In Figure 3 the values of the viscosity-corrected sedimentation coefficients, $\eta_r s^0$, are plotted against the density of the suspending medium, ρ, where η_r is the relative viscosity of the medium. The isodensity value, ρ_i, for the DMPC vesicle bilayer was obtained from a least-squares linear interpolation of the data in Figure 3 at $\eta_r s^0$ = 0 (Huang & Charlton, 1971).

The temperature dependence of the effective partial specific volume, $\phi = 1/\rho_i$, of the DMPC vesicles is compared with the Tempo spin-label indication of the vesicle bilayer phase tran-

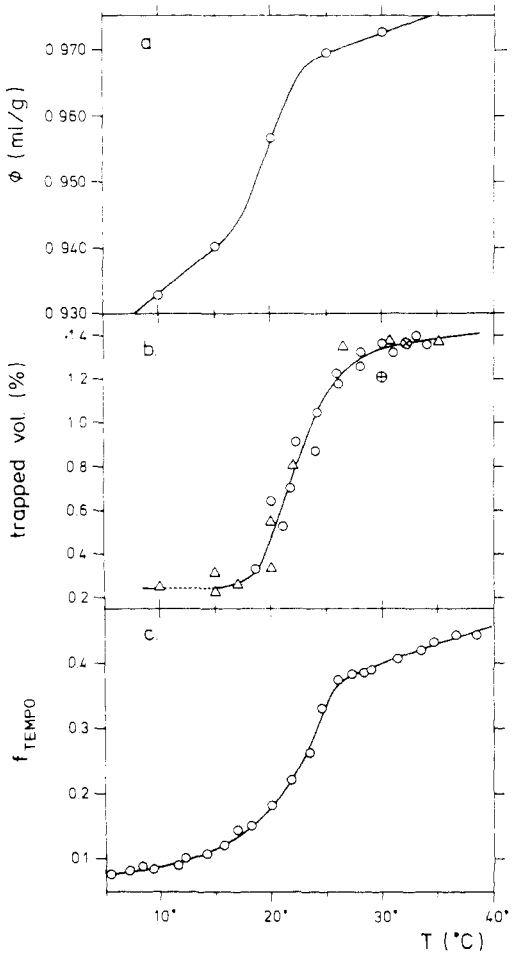

FIGURE 4: (a) Effective partial specific volume, ϕ, of DMPC vesicles vs. temperature. (b) Trapped volume of DMPC vesicles vs. temperature. (○) Limiting uptake of Tempocholine after incubation at different temperatures for 120 min; (△) Tempocholine uptake after brief resonication at various temperatures; (⊗) Tempocholine uptake after cosonication at 30 °C; (⊕) Tempophosphate uptake after cosonication at 30 °C. (c) Fractional partitioning of Tempo spin label into DMPC vesicles vs. temperature (see Marsh et al., 1977).

sition in Figure 4.[2] The quoted error limits of the values of ϕ given in Table I correspond to the standard deviations of the linear least-squares interpolations in Figure 3. Corrected sedimentation coefficients, $s^0_{20,w}$ are given in Table I and were obtained from the data of Figure 3 corresponding to a solvent buffer system containing 100% H_2O. The quoted error limits on $s^0_{20,w}$ correspond to the standard deviations of the least-squares fits to the concentration dependencies of s in Figure 2.

Diffusion Coefficients. The plots of schlieren peak area vs. time for patterns recorded during a diffusion experiment were all linear and least-squares analysis was used to determine the slopes to give the apparent diffusion coefficients, D_{app}, which are plotted in Figure 5 as a function of lipid concentration. A

[2] The phase transition indicated by Tempo is broadened because of the reduced cooperativity in small vesicles relative to extended multibilayers (Marsh et al., 1977). For dipalmitoylphosphatidylcholine vesicles, the transition temperature is also depressed (Marsh et al., 1977; Suurkusk et al., 1976), whereas for DMPC vesicles the transition temperature is only depressed by a small amount if at all (Marsh et al., 1977). The reason for this difference is not known, but it is clear that both the partial specific volume and the internal volume results in Figure 4a,b correlate reasonably well both in transition temperature and width with the Tempo indication of the phase transition. At most, the partial specific volume transition is depressed by 2-3 °C relative to the Tempo transition.

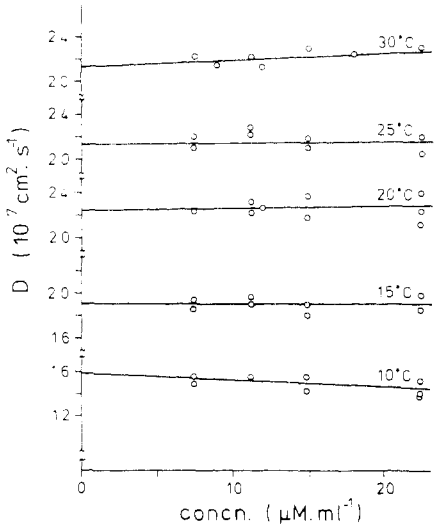

FIGURE 5: Apparent diffusion coefficients, D, of DMPC vesicles vs. concentration at various temperatures. Buffer: H_2O-0.1 M KCl-0.01 M Tris (pH 8.0).

linear least-squares analysis was also used in the extrapolation of the concentration dependence of Figure 5 to give the values of D_{app} at infinite dilution, D^0.

The values of the corrected diffusion coefficients, $D^0_{20,w}$, are given in Table I. The quoted error limits on $D^0_{20,w}$ correspond to the standard deviation of the least-squares fit of the concentration dependence of D in Figure 5.

Trapped Volume Measurements. The temperature dependencies of the internal volume of DMPC vesicles, measured by both the limiting uptake and brief resonication methods, are given in Figure 5b. It is seen that the results from both methods coincide over the temperature range for which both are applicable, and also agree with the values obtained by cosonication with Tempocholine or Tempophosphate at 30 °C. Comparison with the Tempo indication of the phase transition (Figure 5c), clearly shows that the trapped volume decreases abruptly on going down through the phase transition. The values of v_c, the trapped volume in units of mL per g of anhydrous lipid, are given in Table I. Some difficulty was experienced in obtaining equilibration of Tempocholine distribution at 10 °C; thus this point is best considered as an extrapolated value.

Vesicle Molecular Weight. The weight-average vesicle molecular weight can be calculated from the measured sedimentation and diffusion coefficients using the Svedberg equation:

$$M = RTs^0_{20,w}/D^0_{20,w}(1 - \phi\rho_{20,w}) \qquad (1)$$

where R is the universal gas constant, T = 293 K, and $\rho_{20,w}$ = 0.99823 g mL^{-1}. The vesicle partial specific volumes at the particular temperatures used in these calculations are the effective partial specific volumes, ϕ, measured in the buffer solution of these experiments (Huang & Charlton, 1971). The molecular weights obtained in this way are the anhydrous vesicle molecular weights and are independent of the vesicle shape. The values of M are given in Table I from which it can be seen that the vesicle molecular weight remains essentially constant with temperature throughout the phase transition. The mean vesicle molecular weight calculated from Table I is: $M = 1.932 \pm 0.096 \times 10^6$ (weighted mean), and the mean number of lipid molecules per vesicle is $n = M/678 = 2850 \pm 140$.

Vesicle Shape. The freeze-etch electron microscopy above

TABLE I: Solution Properties of Dimyristoylphosphatidylcholine Vesicles.

	Temp (°C)				
	10	15	20	25	30
ϕ (mL/g)	0.9328 ± 0.0014	0.9401 ± 0.0016	0.9565 ± 0.0015	0.9695 ± 0.0012	0.9726 ± 0.0014
$s^0_{20,w}/10^{-13}$ (s)	11.81 ± 0.65	11.69 ± 0.68	7.07 ± 0.26	5.33 ± 0.23	4.40 ± 0.31
$D^0_{20,w}/10^{-7}$ (cm²/s)	2.168 ± 0.085	2.226 ± 0.082	2.236 ± 0.068	1.881 ± 0.113	1.665 ± 0.040
$M/10^6$	1.93 ± 0.22	2.08 ± 0.25	1.71 ± 0.17	2.14 ± 0.30	2.21 ± 0.31
$[\eta]$ (dL/g)	0.02730 ± 0.00016	0.0285 ± 0.0009	0.03122 ± 0.00046	0.04291 ± 0.00087	0.05480 ± 0.00076
v_c (mL/g lipid)	(0.107 ± 0.024)[a]	0.107 ± 0.024	0.240 ± 0.043	0.542 ± 0.020	0.6391 ± 0.0052

[a] Extrapolated value.

TABLE II: Data on Vesicle Shape and Hydration Deduced from Viscometry and Ultracentrifugation.

	Temp (°C)				
	10	15	20	25	30
$\beta/10^6$	2.01 ± 0.11	2.18 ± 0.14	2.08 ± 0.10	2.10 ± 0.15	2.04 ± 0.10
w_t(visc) (g/g lipid)[b]	0.1599 ± 0.0078	0.201 ± 0.038	0.292 ± 0.020	0.745 ± 0.036	1.216 ± 0.032
w_t(diff) (g/g lipid)[c]	0.330 ± 0.196	0.142 ± 0.172	0.343 ± 0.173	0.767 ± 0.347	1.454 ± 0.398
w_t(mean) (g/g lipid)[d]	0.1602 ± 0.0078	0.198 ± 0.037	0.293 ± 0.020	0.746 ± 0.036	1.217 ± 0.032
w_i (g/g lipid)	(0.108 ± 0.024)[a]	0.108 ± 0.024	0.240 ± 0.043	0.541 ± 0.020	0.6373 ± 0.0052
w_e (g/g lipid)	(0.053 ± 0.032)[a]	0.091 ± 0.061	0.053 ± 0.063	0.205 ± 0.056	0.580 ± 0.037

[a] Extrapolated value. [b] From viscosity measurements. [c] From diffusion measurements. [d] Weighted mean of viscosity and diffusion values.

indicated that the vesicles were spherical at temperatures both above and below the phase transition. Information about the vesicle shape can also be obtained from the solution studies; by combining the intrinsic viscosity and diffusion coefficient to eliminate the size-dependent terms, an expression is obtained which depends only on vesicle shape. The appropriate expression is the β function defined by Scheraga & Mandelkern (1953):

$$\beta = D^0_{20,w}[\eta]^{1/3}M^{1/3}\eta_0/kT \quad (2)$$

where k is Boltzmann's constant, $T = 293$ K, $\eta_0 = 0.01002$ P is the viscosity of water at 20 °C, and $[\eta]$ is the intrinsic viscosity of the vesicle suspension, the values of which are given in Table I. The error limits on $[\eta]$ correspond to the standard deviation of the linear, least-squares fit of η_{sp}/c vs. c.

The values of β for the various temperatures are given in Table II. The theoretical value of β for spherical particles is 2.12×10^6, this being the lowest possible value. Any deviation from spherical particle symmetry is indicated by higher values of β. It can be seen from Table II that the value of β for spherical particles lies within the experimental limits for DMPC vesicles at all temperatures measured. Thus the solution studies are in agreement with the finding from electron microscopy that the vesicles are spherical at all temperatures.

Unfortunately the β function is not a very sensitive indicator of particle asymmetry. Further checks are possible by assuming that the vesicles are spherical and then calculating dimensional information, water of hydration (determined by total vesicle volume), and vesicle outer radius, from the diffusion data and from the viscosity data independently. The degree of agreement between the two sets of values is a test both of the assumption that the vesicles are spherical and of the consistency of the experimental measurements. These calculations are performed in the next two sections; in all that follows it is assumed that the vesicles are spherical.

Vesicle Hydration. The total volume of the hydrated vesicle is composed of the lipid bilayer volume plus that of its associated water, both trapped and bound. In terms of specific volumes (Scheraga & Mandelkern, 1953):

$$\bar{V}_h = \phi + w_t/\rho \quad (3)$$

where $\bar{V}_h$ is the total volume of the hydrated vesicle per g of lipid, ϕ is the vesicle effective partial specific volume, w_t is the total mass of water associated with the vesicle in g per g of lipid and ρ is the density of the free aqueous phase. No assumptions are made about the compartmentation of the associated water, nor about its density, in this equation (Yang, 1961).

The total mass of water associated with the vesicle can then be obtained directly from the intrinsic viscosity since (Oncley, 1941)

$$[\eta] = \nu\bar{V}_h/100 \quad (4)$$

where ν, the Simha viscosity increment, is shape dependent and has a value of 2.5 for spherical particles. The values of w_t obtained in this way are listed in Table II.

Calculation using the diffusion coefficient is less direct. The diffusion coefficient is related to the frictional coefficient, f, by the Einstein–Sutherland equation:

$$D = kT/f \quad (5)$$

where k is Boltzmann's constant and T the absolute temperature (Svedberg & Pedersen, 1940). The value of f for a rigid sphere, of radius r_s, is given by the Stokes Law expression:

$$f = 6\pi\eta r_s \quad (6)$$

where η is the viscosity of the suspending medium. If the Stokes radius, r_s, is identified with the radius of the assumed spherical, hydrated vesicle, then $\bar{V}_h = 4\pi N r_s^3/3M$, and the specific volume of the hydrated vesicle can be obtained from the measured frictional coefficient according to:

$$f = 6\pi\eta(3M\bar{V}_h/4\pi N)^{1/3} \quad (7)$$

where M is the vesicle molecular weight and N is Avogadro's number. Values of w_t obtained from eq 3, 5, and 7, using the

TABLE III: Vesicle and Bilayer Dimensions.

	Temp (°C)				
	10	15	20	25	30
r_s (Å)	98.8 ± 3.9	96.2 ± 3.5	95.8 ± 2.9	113.9 ± 6.8	128.7 ± 3.1
r_h (Å)	94.2 ± 3.8	97.9 ± 5.0	94.5 ± 3.7	113.4 ± 6.0	124.3 ± 6.4
r_0 (Å)[b]	96.4 ± 2.7	96.8 ± 2.9	95.3 ± 2.3	113.6 ± 4.5	127.8 ± 2.8
r_i (Å)	(43.4 ± 4.9)[a]	44.5 ± 5.1	54.5 ± 5.1	77.2 ± 4.5	82.4 ± 4.1
r_e (Å)	(92.6 ± 4.3)[a]	95.2 ± 4.6	93.2 ± 4.3	108.7 ± 5.6	112.2 ± 5.4
h (Å)[c]	(3.55 ± 0.72)[a]	1.14 ± 0.47	2.29 ± 0.80	4.8 ± 1.2	13.3 ± 1.0
d_l (Å)	(49.22 ± 0.59)[a]	50.68 ± 0.50	38.64 ± 0.78	31.5 ± 1.0	29.8 ± 1.3
F (Å^2)	(46.2 ± 3.5)[a]	45.3 ± 3.6	58.2 ± 4.7	70.7 ± 4.3	74.7 ± 3.7

[a] Extrapolated value. [b] Weighted mean of r_s and r_h. [c] Weighted mean of values calculated from r_s and r_h separately.

measured values of $D^0_{20,w}$ and T = 293 K, η = 0.01002 P, are given in Table II. Comparison with the values obtained from the viscosity measurements shows agreement within the experimental error, although the differences in some cases are quite large. The weighted mean of the values obtained from viscosity and diffusion measurements is taken as the best value for w_t (Table II).

The above calculations have made no assumption about the density of the associated water. The amount of water, w_i, contained within the internal volume of the vesicle, expressed in g per g of lipid, can be obtained from the measured values of trapped volume, v_c (mL/g of lipid), if it is assumed that the internal aqueous phase has the same density, ρ, as the free buffer:

$$w_i = \rho v_c \tag{8}$$

Values for the amount of water additionally associated with the lipid are then given by the difference

$$w_e = w_t - w_i \tag{9}$$

where w_e is the mass of water, in g per g of lipid, associated with the lipid bilayer in addition to that contained in the trapped volume of the vesicle. The calculated values of w_i and w_e are also given in Table II.

Vesicle Dimensions. The outer radius of the hydrated vesicle can be obtained both from diffusion and from viscosity measurements. The Stokes radius, r_s, can be identified with the vesicle outer radius, and this is obtained directly from the measured diffusion coefficients using eq 5 and 6:

$$r_s = kT/6\pi\eta D \tag{10}$$

Alternatively, the outer radius can be calculated from the specific volume of the hydrated vesicle, $\bar{V}_h$, obtained from the intrinsic viscosity measurements via eq 4. The hydrated radius is then given by:

$$r_h = (3M\bar{V}_h/4\pi N)^{1/3} \tag{11}$$

The values of r_s and r_h obtained from the diffusion and viscosity experiments, respectively, are given in Table III. The two sets of values can be seen to be in quite good agreement, and their weighted mean is taken as the best value for r_0, the outer radius of the vesicle (see Table III).

The internal radius of the vesicle r_i can be obtained directly from the trapped volume measurements:

$$r_i = (3Mv_c/4\pi N)^{1/3} \tag{12}$$

This assumes that the whole of the internal volume is accessible to Tempocholine. The values of r_i calculated at the various temperatures are given in Table III.

Further dimensions, including those of the lipid bilayer, can be calculated if a three-compartment model is assumed for the vesicle (see Figure 6), as was done by Johnson (1973).[3] The measured effective partial specific volume can be expressed in this model by rearranging eq 3:

$$\phi = \bar{v}_l + v_c + v_e - w_t/\rho \tag{13}$$

where $\bar{v}_l$ is the partial specific volume of the anhydrous bilayer lipid alone, v_c is the trapped volume in mL/g of lipid, and v_e is the additional volume of water, in mL/g of lipid, associated with the bilayer. Thus only the quantity $(\bar{v}_l + v_e)$ is directly accessible from the measurements. However, if it is assumed that the density of both the trapped and the bound water is equal to that of the free buffer, then the partial specific volume of the lipid bilayer is simply: $\bar{v}_l = \phi$. The external radius of the lipid bilayer, r_e (see Figure 6), can then be calculated from the anhydrous vesicle molecular weight, together with the trapped volume:

$$r_e = [(3M/4\pi N)(\phi + v_c)]^{1/3} \tag{14}$$

The anhydrous bilayer thickness is then given directly by

$$d_l = r_e - r_i \tag{15}$$

and the thickness of the external bound water layer by

$$h = r_0 - r_e \tag{16}$$

The values of r_e, h, and d_l calculated at the various temperatures are given in Table III.

Knowing the total surface area of both faces of the lipid bilayer and the number of molecules per vesicle, it is then possible to calculate F, the area per lipid molecule in the bilayer:

$$F = 4\pi(r_e^2 + r_i^2)M_l/M \tag{17}$$

where M_l = 678 is the molecular weight of the DMPC molecule and M is the molecular weight of the whole vesicle. In this the additional assumption is made that there is symmetric molecular packing in the two halves of the bilayer. This is probably not the case and this point is considered in more detail in the Discussion section. The calculated values of F with this assumption are given in Table III. The errors quoted in Table III are calculated taking into account the interdependence of errors in eq 14–17. In particular it should be noted that there

[3] In spite of possible asymmetry in packing between the inner and outer monolayers of the vesicle, it is unlikely that there is much difference in density between the two monolayers, since the bilayer phase transition, which produces a dramatic change in lipid packing, is accompanied by only a 2% change in partial specific volume (Träuble & Haynes, 1971). The assumption of a homogeneous partial specific volume throughout the entire bilayer is thus a reasonable model for the vesicle structure.

is partial cancellation of errors in calculating d_1 and h, resulting in smaller absolute errors than those in r_e, r_i, or r_0.

Discussion

Taken together, the column chromatography and electron microscopy results show that the procedure described above has produced a relatively homogeneous population of spherical vesicles which consist of a single bilayer surrounding a separate internal aqueous compartment. The hydrodynamic results indicate that the vesicles maintain this configuration over extended periods of time, at least over the duration of the experiments. Thus no anomalous concentration dependences were observed, the sedimentation peaks remained reasonably symmetrical, and no additional peaks were observed corresponding to fused or aggregated vesicles, throughout the whole of the temperature range studied. Similar results on the stability of the vesicles against fusion have also been obtained previously (Marsh et al., 1976).

The anhydrous vesicle molecular weights calculated in Table I involve no assumptions regarding vesicle shape, size, or hydration and are a direct estimate of the number of lipid molecules per vesicle. The fact that the molecular weight remains constant, to within experimental error, throughout the phase transition again shows that the vesicles are stable over the time scale of the experiments and do not undergo fusion or phospholipid transfer to build bigger vesicles. In contrast the measured effective partial specific volumes undergo an abrupt change at the phase transition, reflecting the molecular changes taking place in the lipid bilayer (Träuble & Haynes, 1971; Marsh, 1974a,b). The change in ϕ between 15 and 25 °C is 0.029 ± 0.003 mL/g, or 3.1%, quite close to the dilatometric value of 0.023 ± 0.003 mL/g reported for the change through the transition in DMPC vesicles (Melchior & Morowitz, 1972). A change in the effective partial specific volume of 3.1%, at the phase transition of sonicated dipalmitoylphosphatidylcholine, has also been reported (Sheetz & Chan, 1972). The absolute values of ϕ below the transition also compare quite well with a calculated value for the partial specific volume of anhydrous DMPC bilayers of $\bar{v}_1 = 0.935$ mL/g (Tardieu et al., 1973), suggesting that the approximation, $\bar{v}_1 = \phi$ used above, was not very much in error.

All the calculations of the vesicle dimensions and hydration, except those of the molecular weight and internal volume of the vesicle, require knowledge of the vesicle shape. These data come from the freeze-etch electron microscopy which shows the vesicles to be spherical at temperatures both above and below the phase transition. Since the freeze-etch electron microscopy faithfully reflects the change in vesicle radius on going through the phase transition found by the viscosity and diffusion measurements, it should also be reliable with respect to the vesicle shape. Calculations from the viscosity and diffusion data, via the β function, are also consistent with a spherical shape. However, to make a definitive statement from viscosity and diffusion measurements would require the data to be much more accurate, because of the insensitivity of the β function to particle asymmetry, especially in the case of oblate spheroids (Yang, 1961). Thus the data on vesicle shape obtained from the electron microscopy is used for the vesicle hydration in Table II and outer and inner radii in Table III, all of which are calculated for spherical vesicles.

To obtain the remaining data in Table III, which essentially concern the properties of the bilayer itself, it is necessary to make some assumption about how the bound water, v_e, is associated with the bilayer. Examination of eq 13 shows that the composite specific volume ($\bar{v}_1 + v_e$) is the only experimentally accessible quantity, and this only permits calculation of the

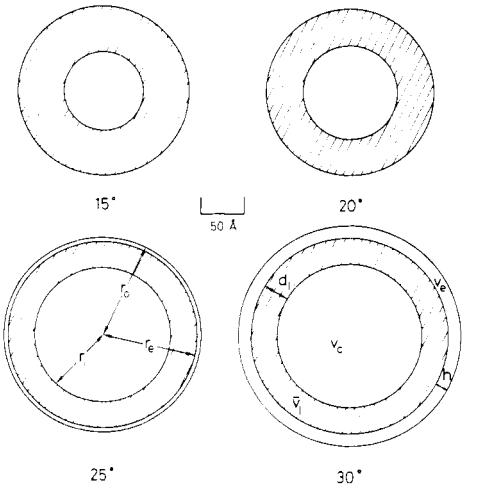

FIGURE 6: Scale diagrams illustrating the dimensional changes in DMPC vesicles through the phase transition. Three compartment model: v_c, vesicle internal volume; $\bar{v}_1$, lipid bilayer; v_e, external bound water layer.

total thickness of the lipid plus bound water layer. The assumption made here is that the whole of the bound water, additional to the trapped volume, is contained in a spherical layer on the vesicle outer surface, as is indicated in the three-compartment model indicated in Figure 6. This assumption is probably not a bad one in view of the hydrophobic nature of the lipid bilayer and the relatively small free volume associated with the polar groups. The additional implicit assumption is that the whole of the internally bound water is accessible to Tempocholine. This is possibly not completely correct, but on the one hand the inaccessible fraction is probably tightly associated with the lipid head groups and so will not appreciably affect the internal radius of the bilayer, and on the other hand the internal surface is much smaller than the external surface, so this fraction probably will not markedly alter the estimation of the outer bound layer.

Examination of the data on bilayer dimensions in Table III gives information both on the configuration of the lipid molecules and on their changes through the phase transition. The bilayer thickness below T_t, $d_1 = 50.7 \pm 0.5$ Å at 15 °C, corresponds closely to the value of 52 Å obtained from molecular models for DMPC molecules with all-trans chains oriented perpendicular to the bilayer, assuming a bent-down head-group conformation and that the glycerol backbone is oriented perpendicular to the bilayer (Seelig & Gally, 1976; Seelig & Seelig, 1975; Hitchcock et al., 1974). A further estimate of bilayer thickness for all-trans chains comes from the partial specific volume: $d_1 = 2M_1\bar{v}_1/NF_0$, where $M_1 = 678$ is the DMPC molecular weight and $F_0 = 40.8$ Å^2 is the area/molecule corresponding to all-trans chains oriented perpendicular to the bilayer. Taking the anhydrous bilayer specific volume, $\bar{v}_1$, as ϕ measured at 15 °C, yields $d_1 = 51.9 \pm 0.1$ Å in good agreement with the measured result and that from molecular models. The measured area/molecule below T_t does not correspond so well with the crystallographic value of $F_0 = 40.8$ Å^2, corresponding to two all-trans chains (Tardieu et al., 1973). However, in highly curved bilayers the definition of molecular area is somewhat ambiguous; the hydrocarbon chain packing is more likely to be determined at the polar–apolar interface than at the polar head-group surface. From molecular models it is seen that the apolar interface occurs at a depth of 5 Å into the bilayer; calculation of the area/molecule at this position yields values of 40.4 ± 3.1 and 39.7 ± 3.2 Å^2 at 10 and 15 °C, respectively. Thus these results suggest that the lipid molecules are predominantly in the all-trans configuration and are ori-

ented close to the bilayer normal, below the phase transition.

The values of d_1 and F in Table III clearly demonstrate that the decrease in bilayer thickness (Janiak et al., 1976) and the lateral expansion (Marsh, 1974b; Träuble & Haynes, 1971), on going through the phase transition, found in extended bilayers occurs also in vesicles. The values of d_1 for the vesicles above T_t compare reasonably well with the x-ray result in extended, DMPC multibilayers, $d_1 = 35$ Å (Janiak et al., 1976), whereas the values for the area/molecule are somewhat higher than the values of $F \sim 60$ Å^2 found in extended bilayer systems (Träuble & Haynes, 1971; Marsh, 1974b). Again, however, if the area/molecule is calculated at the apolar interface one gets $F = 63.5 \pm 3.9$ and 67.4 ± 3.3 Å^2 at 25 and 30 °C, respectively. Thus the vesicle measurements faithfully reflect the known behavior of the lipid bilayer as the molecules fluidize on going through the phase transition and provide the additional information that the lipid molecules are oriented more nearly perpendicular to the vesicle surface below the transition.

Whilst the above considerations have shown that the gross, overall features of the bilayer phase transition are the same as in extended, planar bilayers, clearly the fine details of the packing arrangements will be different in highly curved vesicles. Thus below the phase transition, laser raman studies (Spiker & Levin, 1976; Gaber & Peticolas, 1977) have indicated the presence of some, presumably static, gauche defects in the lipid chains which correlates with the slightly reduced bilayer thickness ($d_1 = 50.7 \pm 0.5$ Å as opposed to 52 Å) observed in the present study. In addition there is evidence for asymmetric molecular packing in the two monolayers of the curved bilayer (Chrzeszczyk et al., 1976; Longmuir & Dahlquist, 1976), although the overall fluidity of the bilayer does not seem to be very different from planar systems (Stockton et al., 1976; Marsh et al., 1972). One possible approach to the problem of asymmetry is suggested by the observation above that the mean area/molecule, averaged over the whole of the vesicle, is comparable to that in extended bilayer systems if one assumes that the surface packing density in the two halves of the bilayer is the same at the glycerol backbone region. Making this and the additional assumption that the partial specific volume is the same in both halves of the bilayer[2] yields different thicknesses for the outer and inner monolayers, 17 and 15 Å, respectively, at 25 °C, and the following results for the area/molecule: 77 and 55 Å^2 for the head and tail regions of the outer monolayer and 62 and 87 Å^2 for the head and tail regions of the inner monolayer, respectively. Thus the bilayer packing asymmetry is seen from the fact that the inner monolayer is thinner and more expanded than the outer monolayer, as found previously in other systems (Chrzeszczyk et al., 1976). Qualitatively similar results may be inferred for the packing below the phase transition, where it must be assumed that static gauche kinks are localized toward the top of the chain in the outer monolayer and close to the end of the chains in the inner monolayer.

The events taking place in the bilayer during the phase transition exert a molecular control on the vesicle size which is depicted in Figure 6. As the bilayer thickness decreases and the area increases, the whole of the vesicle expands. The effect is most marked on the internal dimensions, since this is the sum of both effects; thus the internal radius increases by 37.9 ± 9.1 Å on going from 15 to 30 °C whereas the change in external radius by comparison is only 17.0 ± 10.0 Å and the change in bilayer thickness is 20.9 ± 1.8 Å. Because of the small size of the vesicle this has a dramatic effect on the internal volume; from Table I it can be seen that this actually increases sixfold on going from 15 to 30 °C. If such a volume change were to take place in a cellular system, it could have important functional implications arising from the change in concentration of internal solutes. For instance, it would correspond to a change in internal pH by 0.8 unit, or a change in membrane potential (assuming a single diffusable ion) of up to 45 mV, and could change passive transport rates by up to sixfold. Such small internal volumes are not universally found in living cells, but some intracellular vesicles approach these sizes, and such membrane protrusions may occur transiently in micropinocytosis or "blebbing". Although temperature changes would not normally be responsible for triggering transitions in biological membranes there is abundant evidence from bilayer systems that phase transitions can be triggered isothermally, e.g., by changes in ionic environment, pressure, pH, etc. (Träuble & Eibl, 1974; Träuble et al., 1974; Chapman et al., 1977).

The lipid phase transition also appears to control the amount of bound water associated with the vesicle. Below the transition the amount of bound water is rather small, the values of w_e corresponding quite closely with the values of 0.08–0.1 g/g lipid found for the amount of nonsolvent water in DMPC liposomes at 10–15 °C (Katz & Diamond, 1974). Above the transition, the bound water increases steeply, presumably as a result of lateral expansion in the head-group region. Qualitatively the same effect is observed with the nonsolvent water in DMPC liposomes which has a value of 0.2 g/g lipid at 25 °C but only increases to 0.25–0.3 g/g lipid at 30 °C (Katz & Diamond, 1974). The value found here for w_e at 30 °C agrees reasonably well with the value for egg phosphatidylcholine vesicles of 0.43 g/g lipid at 20 °C (Newman & Huang, 1975) and is comparable with the total amount of motionally restricted water in dipalmitoylphosphatidylcholine multilayers, as determined above the phase transition by deuterium nuclear magnetic resonance (Salisbury et al., 1972). These changes in hydration could also modulate the functional properties of the bilayer. Thus the requirement for a hydration layer has been demonstrated in the phospholipase A_2 attack of phosphatidylcholine molecules (Misiorowski & Wells, 1974), and it has also been postulated that the bound water layer is the limiting barrier to water permeability of phospholipid membranes (Finch & Schneider, 1975).

After submission of this work, Aune et al. (1977) published data on the temperature dependence of the outer radius of a sonicated preparation of DMPC vesicles using quasi-elastic light scattering. In contrast to the present results, no significant change was found in the outer radius over the temperature range 14–34 °C. The discrepancy presumably arises from differences in the two preparations: Aune et al. (1977) found a vesicle weight of 2.73×10^6 whereas that of the present preparation is $1.932 \pm 0.096 \times 10^6$. We are confident of the changes in outer radius reported in the present work since they were obtained by two independent methods, viscosity and diffusion (which have quite different radial dependences), and are supported by electron microscopy.

Acknowledgments

We would like to thank Mr. R. Boyes and Frl. U. Bottin for their excellent technical assistance and Dr. W. T. Wolodko for his help and advice with the analytical ultracentrifugation.

References

Aune, K. C., Gallagher, J. G., Gotto, A. M., & Morrisett, J. D. (1977) *Biochemistry 16,* 2151.

Bangham, A. D., Hill, M. W., & Miller, N. G. A. (1974) in

Methods in Membrane Biology (Korn E. D., Ed.) Vol. 1, Plenum Press, New York, N.Y.
Bates, R. G. (1965) *Determination of pH. Theory and Practice*, Wiley, New York, N.Y.
Chapman, D., Peel, W. E., Kingston, B., & Lilley, T. H. (1977) *Biochim. Biophys. Acta 464,* 260.
Chervenka, C. H. (1969) *A Manual of Methods for the Analytical Ultracentrifuge*, Spinco Division of Beckman Instruments, Palo Alto, Calif.
Chong, C. S., & Colbow, K. (1976) *Biochim. Biophys. Acta 436,* 260.
Chrzeszczyk, A., Wishnia, A., & Springer, C. S. (1976) *ACS Symp. 34,* 483.
Dittmer, J., & Lester, R. L. (1964) *J. Lipid Res. 5,* 126.
Ehrenberg, A. (1957) *Acta Chem. Scand. 11,* 1257.
Eibl, H., & Lands, W. E. M. (1969) *Anal. Biochem. 30,* 51.
Finch, E. D., & Schneider, A. S. (1975) *Biochim. Biophys. Acta 406,* 146.
Gaber, B. P., & Peticolas, W. L. (1977) *Biochim. Biophys. Acta 465,* 260.
Hill, J., & Cox, D. J. (1965) *J. Phys. Chem. 69,* 3032.
Hitchcock, P. B., Mason, R., Thomas, K. M., & Shipley, G. G. (1974) *Proc. Natl. Acad. Sci. U.S.A. 71,* 3036.
Huang, C. (1969) *Biochemistry 8,* 344.
Huang, C., & Charlton, J. P. (1971) *J. Biol. Chem. 246,* 2555.
Huang, C., & Charlton, J. P. (1972) *Biochemistry 11,* 735.
Huang, C., & Lee, L. (1973) *J. Am. Chem. Soc. 95,* 234.
Huang, C., Charlton, J. P., Shyr, C. I., & Thompson, T. E. (1970) *Biochemistry 9,* 3422.
Huggins, M. L. (1942) *J. Am. Chem. Soc. 64,* 2716.
Janiak, M. J., Small, D. M., & Shipley, G. G. (1976) *Biochemistry 15,* 4575.
Johnson, S. M. (1973) *Biochim. Biophys. Acta 307,* 27.
Katz, Y., & Diamond, J. M. (1974) *J. Membr. Biol. 17,* 87.
Kleeman, W., & McConnell, H. M. (1976) *Biochim. Biophys. Acta 419,* 206.
Kornberg, R. D., & McConnell, H. M. (1971) *Biochemistry 10,* 1111.
Langmuir, K. J., & Dahlquist, F. W. (1976) *Proc. Natl. Acad. Sci. U.S.A. 73,* 2716.
Lee, A. G. (1975) *Prog. Biophys. Mol. Biol. 29,* 3.
Levine, Y. K., & Wilkins, M. H. F. (1971) *Nature (London), New Biol. 230,* 69.
Marsh, D. (1974a) *J. Membr. Biol. 18,* 145.
Marsh, D. (1974b) *Biochim. Biophys. Acta 363,* 373.
Marsh, D. (1975) *Essays Biochem. 11,* 139.
Marsh, D., Phillips, A. D., Watts, A., & Knowles, P. F. (1972) *Biochem. Biophys. Res. Commun. 49,* 691.
Marsh, D., Watts, A., & Knowles, P. F. (1976) *Biochemistry 15,* 3570.
Marsh, D., Watts, A., & Knowles, P. F. (1977) *Biochim. Biophys. Acta 465,* 500.
Martin, F. J., & MacDonald, R. C. (1976) *Biochemistry 15,* 321.
Melchior, D. L., & Morowitz, H. J. (1972) *Biochemistry 11,* 4558.
Melchior, D. L., & Steim, J. M. (1976) *Annu. Rev. Biophys. Bioeng. 5,* 205.
Misiorowski, R. L., & Wells, M. A. (1974) *Biochemistry 13,* 4921.
Newman, G. C., & Huang, C. (1975) *Biochemistry 14,* 3363.
Oncley, J. L. (1941) *Ann. N.Y. Acad. Sci. 41,* 121.
Papahadjopoulos, D., & Kimelberg, H. K. (1973) *Prog. Surf. Sci. 4,* 141.
Papahadjopoulos, D., Hui, S., Vail, W. J., & Poste, G. (1976) *Biochim. Biophys. Acta 448,* 245.
Salisbury, N. J., Darke, A., & Chapman, D. (1972) *Chem. Phys. Lipids 8,* 142.
Seelig, A., & Seelig, J. (1975) *Biochim. Biophys. Acta 406,* 1.
Seelig, J., & Gally, H. U. (1976) *Biochemistry 15,* 5199.
Schachman, R. K. (1957) *Methods Enzymol. 4,* 32.
Scheraga, H. A., & Mandelkern, L. (1953) *J. Am. Chem. Soc. 75,* 179.
Schreier-Muccillo, S., Marsh, D., Dugas, H., Schneider, H., & Smith, I. C. P. (1973) *Chem. Phys. Lipids 10,* 11.
Sheetz, M. P., & Chan, S. I. (1972) *Biochemistry 11,* 4573.
Spiker, R. C., & Levin, I. W. (1976) *Biochim. Biophys. Acta 455,* 560.
Stockton, G. W., Polnaszek, C. F., Tulloch, A. P., Hasan, F., & Smith, I. C. P. (1976) *Biochemistry 15,* 954.
Suurkuusk, J., Lentz, B. R., Barenholz, Y., Biltonen, R. L., & Thompson, T. E. (1976) *Biochemistry 15,* 1393.
Svedberg, T., & Pedersen, K. O. (1940) *The Ultracentrifuge,* Oxford University, London.
Tardieu, A., Luzzati, V., & Reman, F. C. (1973) *J. Mol. Biol. 75,* 711.
Taupin, C., & McConnell, H. M. (1972) *Proc. Meet. Fed. Eur. Biochem. Soc. 28,* 219.
Träuble, H., & Eibl, H. (1974) *Proc. Natl. Acad. Sci. U.S.A. 71,* 214.
Träuble, H., & Haynes, D. H. (1971) *Chem. Phys. Lipids 7,* 324.
Träuble, H., Eibl, H., & Sawada, H. (1974) *Naturwissenschaften 61,* 344.
Yang, J. T. (1961) *Adv. Protein Chem. 16,* 323.